

Jet-production mechanism in lepton-hadron reactions

Tetsuro Kitazoe

Department of Physics, Kobe University, Kobe, Japan

Toshiyuki Morii

College of Liberal Arts, Kobe University, Kobe, Japan

(Received 15 August 1979)

A strong Lorentz-contraction effect of the wave function inside every incoming or outgoing hadron is taken into account in lepton-hadron reactions to understand materialization processes to form jets. A formation of only two jets is derived as a result of coordination of the strongly contracted wave functions. The formalism manifests two distinct models. The one is a strongly ordered cascade model which is in accord with a naive quark-parton cascade model. The other is an uncorrelated jet model which is in accord with an uncorrelated Monte Carlo calculation and it cannot be described as a cascade. Several observable quantities are presented to discriminate between these two models. A space-time evolution in materialization is studied and shown to correspond to an "inside-outside" process.

I. INTRODUCTION

Although a naive quark-cascade description^{1,2} seems to be quite successful in high-energy reactions, there still remain ambiguous situations around "materialization." What mechanism underlies the quark-jet generation?² It seems important to study the processes in detail where "real" or "almost real" quarks are produced and decay into themselves emitting hadrons, keeping conservation of energy-momentum. There have been several theoretical attempts³ to understand the dynamical situation in materialization processes and jet production in $e^+ + e^- \rightarrow$ hadrons, lepton-hadron, and other high-energy reactions. We would like to present here a simple mechanism of jet formation in lepton-hadron reactions by paying specific attention to the space-time structure inside a hadron.

We use a Bethe-Salpeter (BS) amplitude to represent a quark bound system inside a hadron. The BS amplitude or wave function has been used to get an understanding of the inclusive reactions.⁴ In this paper, we consider the exclusive reactions and apply the BS amplitude to every hadron, incoming or outgoing, concerned in a reaction. When a production amplitude of a certain Feynman diagram is written down in terms of the BS amplitudes of incoming and outgoing hadrons, the production matrix element is represented by an overlap integral of all the BS amplitudes. It is assumed that a confinement potential localizes quarks in a finite region inside a hadron at rest. When a hadron moves with very high energy, the localized region is strongly deformed by a Lorentz contraction⁵ and crushed onto a line along a light cone whose three-dimensional direction is parallel to the center-of-mass momentum. The overlap

integral becomes large when the deformed region of every BS amplitude has a similar form along a certain direction with a common area. Thus we obtain a crude understanding of the jet-formation mechanism, since the direction of the deformation is intimately related to the center-of-mass momentum of a hadron.

In the previous paper,⁶ remarkable success was obtained in understanding jet structure of $e^+e^- \rightarrow$ hadrons processes on this basis. We adopted a loop diagram to calculate the overlap integral. Here we apply the same formalism to lepton-hadron reactions where jets have been observed recently.⁷ Though we actually discuss lepton-meson scatterings, essential points remain unchanged for lepton-nucleon reactions.⁸ Since we have less knowledge about higher-order perturbation effects in quantum chromodynamics, we consider a loop diagram⁹ assuming that gluons cannot carry much momenta between high-energy virtual quarks.¹⁰ We study what physical consequences result from this assumption.

It is shown that this formalism leads to a simple understanding of narrow-jet production processes with only two jets. Two distinct models are describable in the formalism where a key role is played by a certain parameter ξ which is related to the original form of the localized region inside a hadron at rest. For small ξ , we have a strongly ordered cascade model which is fairly well in accord with the naive quark-parton cascade model.¹ A materialization process is described there as a stochastic process in a quark-cascade decay. For larger ξ , the cascade description fails to work because interference terms between different Feynman diagrams should be taken into account. For large enough ξ , we arrive at another simple model where each interfering term has

equal weight and final-meson momenta have a weak correlation. This model is called the uncorrelated jet model¹¹ which is in accord with an uncorrelated Monte Carlo calculation¹² in the longitudinal phase volume.

The strongly ordered cascade model leads to an equal-spacing distribution of the final-hadron momenta in rapidity space. The uncorrelated jet model leads to a symmetric distribution among the final-hadron momenta in the Feynman x variables. The real world may be intermediate between these two distinct models. In order to discriminate between these two models, several observables are presented to see which model experimental data will favor. When an overlap integral is expressed in terms of space-time variables, we can trace the space-time development in the materialization process. Though a loop diagram looks like an "outside-inside" process, a detailed study shows that the development corresponds to an "inside-outside" process,³ which gives a reasonable account of the materialization process, rather than to an "outside-inside" one.

This paper is organized as follows. Section II is devoted to a qualitative understanding of jet structure and to the calculation of the overlap integral. In Sec. III, two distinct models are derived and we discuss separately the strongly ordered cascade model and the uncorrelated jet model. In Sec. IV, the space-time evolution of the materialization process is discussed. In Sec. V, several observables to distinguish between the two models are proposed. Section VI is devoted to discussions and conclusions.

II. JET STRUCTURE AND OVERLAP INTEGRAL

Let us begin with the definition of the bound-state BS amplitude and consider its Lorentz contraction at high energy which plays a central role in jet formation. A meson BS amplitude of $q\bar{q}$ system is defined in relative-momentum (k) space as

$$\chi_{\alpha\beta}^{ab}(p, k) = \sqrt{2E}(2\pi)^{3/2} \int d^4x e^{ik \cdot x} \times \langle M | T \bar{\psi}_{\beta}(\frac{1}{2}x) \psi_{\alpha}(-\frac{1}{2}x) | 0 \rangle, \quad (2.1)$$

where $\langle M |$ represents a one-meson state with momentum \vec{p} and other quantum numbers, and ψ_{α}^a is a quark field with spinor index α and color-flavor index a . χ splits into spinor part S , flavor \otimes color part $\Lambda^{(3)} (\equiv \lambda^{(3)} \otimes 1)$, and a function F in relative-momentum space as

$$\chi_{\alpha\beta}^{ab} = \Lambda_{ab}^{(i)} S_{\alpha\beta}(p) F(k^2, p \cdot k) \quad (2.2)$$

for an S-wave bound state.

We pay special attention to the Lorentz con-

traction of F . Suppose a confinement potential localizes the BS amplitude F in a finite region of the relative-momentum space inside a meson. Since an S-wave ground-state wave function is spherical symmetric and has no nodes, the finite region is approximated to an ellipse with radii Δ and $\beta\Delta$ in relative-momentum and energy space, respectively. When a meson moves with high speed, the region is strongly crushed onto a light cone with the volume kept conserved⁶;

$$(k^2)_p \equiv [(1 + \beta^2)(p \cdot k)^2 / \beta^2 m^2 - k^2] / \Delta^2 = (k_0 + k_{||})^2 / 2D_L^2 + (k_0 - k_{||})^2 / 2D_S^2 + \vec{k}_{\perp}^2 / \Delta^2 \leq 1, \quad (2.3)$$

where m is meson mass, and k_0 , $k_{||}$, and \vec{k}_{\perp} are energy, longitudinal, and transverse components of the relative momentum k , respectively. The function F which is dominant in this region might be expressed as

$$F(k^2, p \cdot k) = f((k^2)_p), \quad (2.4)$$

where $f(x)$ has a mean range $x=1$. Since the long radius D_L and short radius D_S are given by

$$D_L = \{\Delta[2(1 + \beta^2)]^{1/2} / m\} |\vec{p}| \equiv \xi |\vec{p}|, \quad (2.5)$$

$$D_S = \{m\beta\Delta / [2(1 + \beta^2)]^{1/2}\} / |\vec{p}| \equiv \eta / |\vec{p}|,$$

the larger the hadron momentum $|\vec{p}|$, the more strongly the elliptic region is crushed¹³:

$$D_S / D_L = \beta m^2 / [2(1 + \beta^2) |\vec{p}|^2] \leq m^2 / (4 |\vec{p}|^2) \ll 1.$$

When one puts $p=1$ GeV/ c and $m=m_{\pi}$, for example, we have $D_S / D_L \leq \frac{1}{200}$. Any slight change of the finite region at rest system from an ellipse does not matter because the strongly crushed region on a light cone has a similar form and is well approximated to an ellipse.

This strong Lorentz contraction leads to an interesting phenomenon when one picks up a virtual-meson production process

$$q(K_{i-1}) - q(K_i) + M(p_i) \quad (2.6)$$

from a certain Feynman diagram. The quark and meson four-momenta are related to the relative momentum k_i as

$$k_i = (K_{i-1} + K_i) / 2 = K_{i-1} - p_i / 2.$$

Since $p_{i0} \simeq |\vec{p}_i|$ at high energies and Eq. (2.3) shows that k_i lies along the light cone very closely as $k_{i0} \simeq k_{i||}$, we obtain

$$k_i \parallel K_{i-1} \parallel K_i \parallel p_i. \quad (2.7)$$

This leads to an important conclusion: The virtual quarks which are related to the meson formation are lightlike (on zero mass shell) and their four-momenta are almost parallel to the emitted meson

momentum.

One may consider a loop diagram⁹ (Fig. 1) if gluons cannot carry much momenta between virtual quarks.¹⁰ Consider lepton-meson reactions as an example. The essential points remain unchanged for lepton-nucleon cases.⁸ We take a high-speed reference frame, say, the center-of-mass system (c.m.s.) of the outgoing hadronic system with high energy W , so that all hadron wave functions are crushed onto a light cone. Using $K_0 \parallel \vec{p}$ in Fig. 1, the four-momenta K_0 , \bar{K}_0 of "primary" virtual quarks $q(K_0)$, $\bar{q}(\bar{K}_0)$ are given by

$$K_0 = (W/2)(1, -\vec{e}), \quad \bar{K}_0 = (W/2)(1, \vec{e}), \quad (2.8)$$

due to $p+q=K_0+\bar{K}_0$, $K_0 \parallel p$, and the lightlike property of K_0, \bar{K}_0 , where $\vec{e} = \vec{q}/|\vec{q}|$ is the direction of " γ ." Here the incident meson enters left next to the " γ " line in Fig. 1.

The "first" step process $q(K_0) \rightarrow q(K_1) + M(p_1)$ in Fig. 1 proceeds with a linear relation $K_1 \parallel p_1 \parallel K_0$ due to Eq. (2.7) and similarly $\bar{q}(\bar{K}_0) \rightarrow \bar{q}(\bar{K}_1) + M(\bar{p}_1)$ with $\bar{K}_1 \parallel \bar{p}_1 \parallel \bar{K}_0$. The sequence of these "decay" processes produces two jets; one has the momentum direction parallel to \vec{q} (" γ " jet) and the other parallel to \vec{p} (T jet). The T jet (" γ " jet) terminates by emitting n_1 (n_2) mesons with a quark $q(K_{n_1})$ ($\bar{q}(\bar{K}_{n_2})$) being left. Since $q(K_{n_1})$ and $\bar{q}(\bar{K}_{n_2})$ are identical in Fig. 1, we have $K_{n_1} = \bar{K}_{n_2} = 0$ due to $K_{n_1} = \bar{K}_{n_2}$, $K_{n_1} \parallel K_0$, and $\bar{K}_{n_2} \parallel \bar{K}_0$.

Let us go into more detail. The Feynman diagram is represented in terms of trace factors T_μ in spinor, flavor, and color space and an overlap integral O_n (Ref. 6);

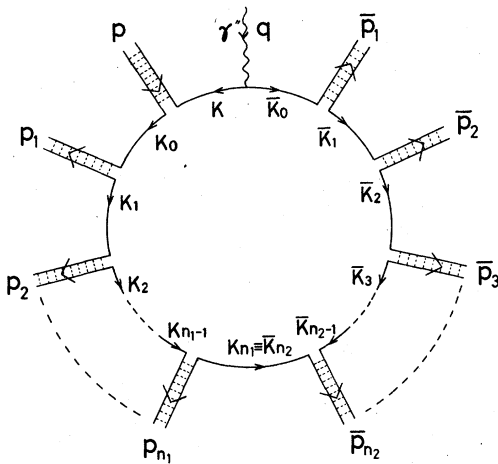


FIG. 1. Quark-loop diagram for n -meson production in a lepton-meson scattering. $q, p, p_i (\bar{p}_i), K, K_i (\bar{K}_i)$ denote respective momenta of the external or internal lines ($K_{n_1} = \bar{K}_{n_2} = 0$). " γ " denotes a virtual photon or weak boson.

$$\langle nM | j_\mu(0) | \vec{p} \rangle = T_\mu O_n / \sqrt{E} \prod_{i=1}^n \sqrt{E_i}. \quad (2.9)$$

O_n is given by

$$O_n = \int dK f((k^2)_p) f((k_1^2)_{p_1}) \times f((k_2^2)_{p_2}) \cdots f((k_n^2)_{p_n}), \quad (2.10)$$

where $p_n = \bar{p}_1, p_{n-1} = \bar{p}_2, \dots, p_{n_1+1} = \bar{p}_{n_2}$. Since $k = K + p/2, k_1 = K + p - p_1/2, k_2 = K + p - p_1 - p_2/2, \dots$, K in Fig. 1 is only one integral variable of O_n . The elliptic region of the incident meson lies along the OA line with a center $-\frac{1}{2}p$ in K space in Fig. 2. The region is hereafter called a tunnel with length $\xi |\vec{p}|$, width $\eta/|\vec{p}|$, and height Δ . If the next tunnel is made by the "first" meson with p_1 along the AB line with a center $-p + p_1/2$ ($\vec{p} \parallel \vec{p}_1$), the overlap of $f((k^2)_p) f((k_1^2)_{p_1})$ becomes large. The sequence of tunnels is made along the AB line. Their centers proceed from A to B by a step $\frac{1}{2}(p_{i-1} + p_i)$. When a sum $\sum_{i=1}^{n_1} p_i$ reaches point B with a certain n_1 , the next tunnel turns to the right at right angles and subsequent tunnels are made along the BC line until $\sum_{i=n_1+1}^n p_i = BC$ is satisfied, which results in energy-momentum conservation, $p+q = \sum_{i=1}^n p_i$. Thus, we obtain two jets along AB (T jet) and BC (" γ " jet). When each direction of the tunnels deviates from \vec{p} or \vec{q} axis, O_n will be reduced. The allowed deviation may have an order of magnitude Δ which is the height of each tunnel;

$$p_1 \sim \Delta. \quad (2.11)$$

This corresponds to the mean value of p_1 distri-

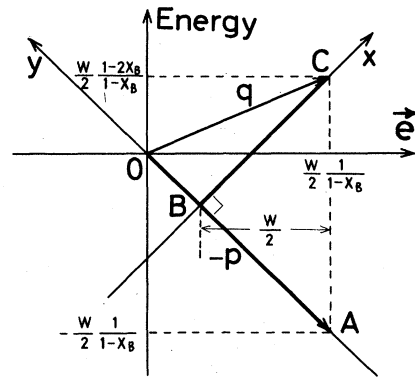


FIG. 2. Momentum diagram corresponding to Fig. 1. $AO = p$ and $OC = q$ represent four-momenta of the incident meson and " γ " in the c.m.s., respectively. $x_B = -q^2/2mv$ is Bjorken's scaling variable. The produced meson momenta lie along AB or BC with $AB = K_0 = \sum_i p_i = (W/2)(1, -\vec{e})$ and $BC = \bar{K}_0 = \sum_i \bar{p}_i = (W/2)(1, \vec{e})$, where $\vec{e} = \vec{q}/|\vec{q}|$. The incident meson's tunnel lies along the OA line and the outgoing meson's tunnels lie along AB and BC in K space.

butions.

The overlapping of each BS amplitude takes place around the point B in a small region where two series of tunnels cross orthogonally. To see this, we change variables p_i 's into

$$\begin{aligned} p_1 &= (W/2)\alpha_1, \quad p_2 = (W/2)(1 - \alpha_1)\alpha_2, \dots, \\ p_{n_1-1} &= (W/2)(1 - \alpha_1)(1 - \alpha_2) \cdots (1 - \alpha_{n_1-2})\alpha_{n_1-1}, \\ p_{n_1} &= (W/2)(1 - \alpha_1)(1 - \alpha_2) \cdots (1 - \alpha_{n_1-1}), \quad (2.12) \\ \bar{p}_1 &= (W/2)\bar{\alpha}_1, \quad \bar{p}_2 = (W/2)(1 - \bar{\alpha}_1)\bar{\alpha}_2, \dots, \\ \bar{p}_{n_2-1} &= (W/2)(1 - \bar{\alpha}_1)(1 - \bar{\alpha}_2) \cdots (1 - \bar{\alpha}_{n_2-2})\bar{\alpha}_{n_2-1}, \\ \bar{p}_{n_2} &= (W/2)(1 - \bar{\alpha}_1)(1 - \bar{\alpha}_2) \cdots (1 - \bar{\alpha}_{n_2-1}), \end{aligned}$$

with $\sum_i p_i = \sum_i \bar{p}_i = W/2$ satisfied. Here, and hereafter, we use p_i to represent $p_{i||}$ or a four-momentum without creating confusion. $(k^2)_p$ and $(k_i^2)_{p_i}$ are given as

$$\begin{aligned} (k^2)_p &= \frac{2}{\xi^2} (x_B - \frac{1}{2})^2 + \frac{p^2}{\eta^2} x^2 + \frac{\bar{K}_1^2}{\Delta^2}, \\ (k_i^2)_{p_i} &= \frac{2}{\xi^2} \left(\frac{1}{\alpha_i} - \frac{1}{2} \right)^2 + \frac{p_i^2}{\eta^2} x^2 + \frac{\bar{K}_1^2}{\Delta^2}, \quad 1 \leq i \leq n_1 \\ (k_i^2)_{\bar{p}_i} &= \frac{2}{\xi^2} \left(\frac{1}{\bar{\alpha}_i} - \frac{1}{2} \right)^2 + \frac{\bar{p}_i^2}{\eta^2} y^2 + \frac{\bar{K}_1^2}{\Delta^2}, \quad 1 \leq i \leq n_2 \end{aligned} \quad (2.13)$$

with $\alpha_{n_1} = \bar{\alpha}_{n_2} = 1$. It is noted that the new variables $x = (K_0 + K_{||})/\sqrt{2}$, $y = \overline{OB} + (K_0 + K_{||})/\sqrt{2}$ and \bar{K}_1 in the integrand of Eq. (2.10) run a very small region around B .

We can carry out the overlap integral around B in a kind of saddle-point approximation,

$$f((k^2)_p) = \exp\{\ln f((k^2)_p)\} \cong f(0) \exp(-(k^2)_p)$$

[note $f'(0)/f(0) = -1$];

$$O_n \cong C_n \exp\left\{-\frac{2}{\xi^2} \left[\sum_{i=1}^{n_1} \left(\frac{1}{\alpha_i} - \frac{1}{2} \right)^2 + \sum_{i=1}^{n_2} \left(\frac{1}{\bar{\alpha}_i} - \frac{1}{2} \right)^2 \right]\right\}, \quad (2.14)$$

$$\begin{aligned} C_n &= [f(0)]^{n+1} \frac{(\pi\Delta\eta)^2}{n+1} \left(p^2 + \sum_{i=1}^{n_1} p_i^2 \right)^{-1/2} \left(\sum_{i=1}^{n_2} \bar{p}_i^2 \right)^{-1/2} \\ &\quad \times \exp[-(2/\xi^2)(x_B - \frac{1}{2})^2]. \end{aligned}$$

The approximation in Eq. (2.14) is reasonable in the region $\alpha_i \geq \alpha_0$, $\bar{\alpha}_i \geq \alpha_0$ with α_0 defined by the relation

$$\alpha_0 = 1/(\frac{1}{2} + \xi/\sqrt{2}) = 1/[\frac{1}{2} + \Delta(1 + \beta^2)/m].$$

Note that this condition is the same one so that the crossed point B in Fig. 2 should be included in every ellipse, $1/\alpha_i - \frac{1}{2} \leq \xi/\sqrt{2}$.

III. FINAL-MOMENTUM DISTRIBUTION

In this section, we discuss the final-hadron's momentum distribution predicted by Eq. (2.14).

Since $\Delta \approx \langle p_{\perp} \rangle$ is not an exact relation, we have to consider two cases. One is the case where α_0 takes rather large values satisfying the relation $\alpha_0 \geq \frac{1}{2}$. (If we set, for example, $\Delta \approx \langle p_{\perp} \rangle \approx m_{\pi}$ and $\beta \approx 0$, we have $\alpha_0 \approx 0.52$.) Since all $\alpha_i, \bar{\alpha}_i$ are more likely to take values larger than $\frac{1}{2}$ in this case, we have strongly ordered final-momentum distributions¹⁴;

$$\begin{aligned} p_1 &> p_2 > p_3 > \cdots > p_{n_1}, \\ \bar{p}_1 &> \bar{p}_2 > \bar{p}_3 > \cdots > \bar{p}_{n_2}. \end{aligned} \quad (3.1)$$

Here we do not have any interference among the final quantum states. Thus we can hopefully treat the production process as a stochastic one which corresponds to a naive parton-cascade model. We call this case the strongly ordered cascade model (SOCM).

If α_0 is much smaller than $\frac{1}{2}$ (ξ is large), on the other hand, $\alpha_i, \bar{\alpha}_i$ can take small values and the final momenta do not follow the strong ordering distributions. (For $\Delta \approx \langle p_{\perp} \rangle \approx 2m_{\pi}$ and $\beta \approx 3$, we have $\alpha_0 \approx 0.11$, $\xi \approx 9$.) In this case, we have to take into account the interference terms among many different Feynman diagrams which come from any allowed interchange of final hadrons.

A. Strongly ordered cascade model (SOCM)

The model where α_0 is large ($\geq \frac{1}{2}$) with small ξ does not have much interference among final momentum states and corresponds to the naive parton-cascade model. The production cross section is proportional to an absolute square of an amplitude. The scaling variable α_i represents a momentum fraction of a daughter meson to the mother quark in a virtual process $q(K_{i-1}) \rightarrow q(K_i) + M(p_i)$; $\alpha_i = p_i/K_{i-1}$. The function $\exp[-(4/\xi^2)(1/\alpha_i - \frac{1}{2})^2]$ is understood to correspond to a decay probability in this process. Since the trace factor T_{μ} does not bring much dependence on each meson momentum in the strong ordering limit¹⁴ (see Sec. VI), the decay function $\Gamma(\alpha)$ in α space is given by

$$\Gamma(\alpha) = \frac{C}{\alpha(1-\alpha)} \exp[-(4/\xi^2)(1/\alpha - \frac{1}{2})^2], \quad (3.2)$$

after the longitudinal phase volume of the final meson states is expressed in terms of α_i 's.⁶ The production cross section is proportional to

$$d\sigma \propto |C_n|^2 \prod_i \Gamma(\alpha_i) d\alpha_i, \quad (3.3)$$

where C_n is approximated in the strong ordering limit¹⁴ to

$$\begin{aligned} C_n &= [f(0)]^{n+1} \frac{1}{n+1} (2\pi\Delta\eta/W)^2 (1-x_B) \\ &\quad \times [1 + (1-x_B)^2]^{-1/2} \exp[-(2/\xi^2)(x_B - \frac{1}{2})^2]. \end{aligned} \quad (3.4)$$

Γ has a scaling property which is in accord with the usual cascade model. There is, however, no guarantee in field theory for Γ to be normalized so that it might be a decay probability. It is a sharply increasing function as $\alpha \rightarrow 1$, ensuring that strong ordering is well satisfied. Thus, we have less quantum-mechanical interference among the final hadron states, which enables us to make a classical description, i.e., a cascade interpretation for Γ . In other words, any decay function Γ should be such a function that it guarantees the strong ordering, as far as we have a cascade description on the field-theoretical basis.

B. Uncorrelated jet model (UCJM)

When α_0 is small and ξ is large, on the other hand, we have to consider a large number of diagrams at the same time to take into account interference effects. Here we consider an extreme case where ξ is very large and the trace factor (T_μ) does not bring much energy dependence. Then, the production amplitude becomes simple, since the exponential factor in Eq. (2.14) is approximately unity except for very small α_i . C_n is given as

$$p(n_c, n_0) = \begin{cases} 2^{-n_0/2} \sum_{k=0}^{n_0} (-1)^k \begin{bmatrix} \frac{n_c}{2} + k \\ k \end{bmatrix} \begin{bmatrix} \frac{n_c}{2} + n_0 - k \\ n_0 - k \end{bmatrix}, & n_c = \text{odd}, \\ 2^{-n_0/2} \sum_{k=0}^{n_0} (-1)^k \begin{bmatrix} \frac{n_c}{2} + k - 1 \\ k \end{bmatrix} \begin{bmatrix} \frac{n_c}{2} + n_0 - k \\ n_0 - k \end{bmatrix}, & n_c = \text{even}. \end{cases} \quad (3.6)$$

This results in

$$p(n_c, n_0) = \begin{cases} 0, & n_c = \text{odd}, n_0 = \text{odd} \\ 2^{-n_0/2} \begin{bmatrix} \frac{n_c}{2} + \frac{n_0}{2} \\ \frac{n_0}{2} \end{bmatrix}, & \text{others.} \end{cases} \quad (3.7)$$

It is notable that $p(n_c, n_0)$ vanishes in an $n_c = \text{odd}$, $n_0 = \text{odd}$ case. This is explained as follows. The final pion states are in $I=0$ and/or $I=1$ states and symmetric in momentum distributions. Bose statistics require that isospin states should be totally symmetric. $n_c = \text{odd}$, $n_1 = \text{odd}$ means that the state is pure $I=1$ and cannot be totally symmetric. Therefore it contradicts Bose statistics. The cross section is proportional to $|C_n|^2$ and $[p(n_c, n_0)]^2$ as

$$d\sigma \propto [p(n_c, n_0)]^2 |C_n|^2 \quad (\text{phase volume}). \quad (3.8)$$

$$C_n \cong [f(0)]^{n+1} \frac{(\pi\Delta\eta)^2}{n+1} \times \frac{1}{\left(\frac{W}{2}\right)^2 \left[\left(\frac{1}{1-x_B}\right)^2 + \sum_i x_i^2\right]^{1/2} (\sum_i \bar{x}_i^2)^{1/2}}, \quad (3.5)$$

where Feynman variables x_i, \bar{x}_i are introduced as $p_i = (W/2)x_i$, $\bar{p}_i = (W/2)\bar{x}_i$. Since C_n is symmetric for any interchange $x_i \leftrightarrow x_j$ ($\bar{x}_i \leftrightarrow \bar{x}_j$), each Feynman diagram which comes from a possible interchange of external mesons attached to the quark line in the "γ" (T)-jet part has an equal contribution to the cross section. Then the cross section depends on the number of independent diagrams. Consider the neutrino-hadron reaction as an example where a u quark kicked by a neutrino produces a "γ" jet. Let n_c and n_0 represent numbers of charged and neutral pions in the "γ" jet, respectively. (We assume that the "γ" jet is composed of pions alone.) The SU(2) factor in isospin space is 1 for $u \rightarrow \pi^+ + d$ and $d \rightarrow \pi^0 + u$ vertices, $1/\sqrt{2}$ for $u \rightarrow \pi^0 + u$ and $-1/\sqrt{2}$ for $d \rightarrow \pi^0 + d$. If odd numbers of π^0 attach to d , the SU(2) factor gives a minus sign relative to the case where even numbers of π^0 attach to d . The sum of independent diagrams which contain these SU(2) factors is given by

The meson momenta are distributed symmetrically along the jet axis in x_i, \bar{x}_i space. Equation (3.7) is a direct result of the assumption that T_μ is symmetric in x_i . Though it is not certain whether this assumption really works in lepton-nucleon scattering or not, the above example is employed to show that we can calculate the production amplitude in the extreme interference case. This case is called the uncorrelated jet model (UCJM)¹¹ which is very close to the uncorrelated Monte Carlo calculation (UMC).¹²

Two distinct models, the SOCM and UCJM, are two extreme cases in between which the real jet phenomena might exist. A numerical estimation shows that the SOCM is well satisfied in the case where $\xi \leq 4$ and the UCJM is well satisfied in the case where $\xi \geq 8$. It is interesting to observe which model the real world is closer to. In Sec. V, several observable quantities to discriminate between these two models are considered.

IV. SPACE-TIME DESCRIPTION

There have been two alternative discussions on the space-time development in the materialization processes. One is an "inside-outside" development and the other is an "outside-inside" one.³ Though the loop diagram we have adopted here looks like the latter process, detailed examination shows that our process belongs to the former category. We illustrate it by considering $e^+ + e^- \rightarrow n$ mesons for simplicity, since a similar discussion is easily applied to lepton-hadron reactions.

First of all, we consider the process in momentum space. The overlap condition of each meson wave function in $e^+ + e^- \rightarrow n$ mesons leads to a jet interpretation. The virtual " γ " at rest with energy W creates $q(K_0)$ and $\bar{q}(\bar{K}_0)$ with lightlike momenta $K_0 = (W/2)(1, -\vec{e})$ and $\bar{K}_0 = (W/2)(1, \vec{e})$, where \vec{e} is a unit vector along a jet axis. These quarks and antiquarks cause two jets through the virtual processes

$$q(K_0) \rightarrow q(K_1) + M(p_1), \quad q(K_1) \rightarrow q(K_2) + M(p_2), \dots,$$

$$q(K_{n-1}) \rightarrow q(K_n) + M(p_n)$$

and

$$\bar{q}(\bar{K}_0) \rightarrow \bar{q}(\bar{K}_1) + M(\bar{p}_1), \quad \bar{q}(\bar{K}_1) \rightarrow \bar{q}(\bar{K}_2) + M(\bar{p}_2), \dots,$$

$$\bar{q}(\bar{K}_{n-1}) \rightarrow \bar{q}(\bar{K}_n) + M(\bar{p}_n).$$

All four-momenta K_i, p_i line up parallel to K_0 , and \bar{K}_i, \bar{p}_i line up parallel to \bar{K}_0 , with the final-quark momentum $K_n = \bar{K}_n = 0$. Since $M(p_i)$ [$M(\bar{p}_i)$] is composed of $q(K_{i-1})\bar{q}(-K_i)$ [$\bar{q}(\bar{K}_{i-1})q(-\bar{K}_i)$] in the

$$\begin{aligned} & (2\pi)^4 O_n \delta^4 \left(q - \sum_{i=1}^{n_1} p_i - \sum_{i=1}^{n_2} \bar{p}_i \right) \\ &= \int g_{p_1}(x_0 - x_1) g_{p_2}(x_1 - x_2) \cdots g_{p_{n_1}}(x_{n_1-1} - x_{n_1}) g_{\bar{p}_1}(x_0 - \bar{x}_1) g_{\bar{p}_2}(\bar{x}_1 - \bar{x}_2) \cdots g_{\bar{p}_{n_2}}(\bar{x}_{n_2-1} - x_{n_1}) \\ & \quad \times \exp \left\{ i \left[-qx_0 + \frac{1}{2}p_1(x_0 + x_1) + \frac{1}{2}p_2(x_1 + x_2) + \cdots + \frac{1}{2}\bar{p}_1(x_0 + \bar{x}_1) + \frac{1}{2}\bar{p}_2(\bar{x}_1 + \bar{x}_2) + \cdots \right] \right\} \\ & \quad \times dx_0 dx_1 dx_2 \cdots dx_{n_1} d\bar{x}_1 d\bar{x}_2 \cdots d\bar{x}_{n_2-1}, \end{aligned} \quad (4.1)$$

where

$$g_p(x) = \frac{1}{(2\pi)^4} \int e^{-ikx} f((k^2)_p) dk. \quad (4.2)$$

Since $f((k^2)_p)$ has a large value in the narrow region of Eq. (2.3), $g_p(x)$ has a significant value in the following region by uncertainty principle

$$(t + x_{i1})^2 / (2p^2/\eta^2) + (t - x_{i1})^2 / (2/\xi^2 p^2) + \Delta^2 \bar{x}_1^2 \leq 1. \quad (4.3)$$

Therefore the region lies along the light cone parallel to p . In order that the integral of Eq. (4.1) has a significant value by overlapping,

$$(x_0 - x_1) \parallel (x_1 - x_2) \parallel \cdots \parallel (x_{n_1-1} - x_{n_1}) \parallel p_1 \parallel p_2 \parallel \cdots \parallel p_{n_1}$$

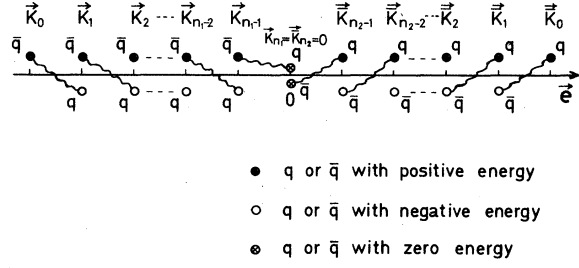


FIG. 3. Particle-hole diagram in momentum space in the one-loop diagram for $e^+e^- \rightarrow n$ mesons reaction. \vec{e} denotes the unit vector along a jet axis. If particles (holes) in the right side are quarks (antiquarks), particles (holes) in the left side are antiquarks (quarks), or vice versa. A particle and a hole connected by a wavy line compose a meson.

Feynman diagram, we illustrate in Fig. 3 three-dimensional momenta of all q, \bar{q} which are produced in the reactions. The figure shows that the vacuum dissociates into pairs of a particle and its hole, where a particle (black circle in Fig. 3) denotes a quark or antiquark with positive energy and a hole (white circle) denotes one with negative energy. A pair of the neighboring particle and hole begins to interact with each other to form a meson.

Next, to see the space-time development we make the Fourier transformation of every wave function in the overlap integral [which is Eq. (2.10) in lepton-meson scattering case] in e^+e^- scattering.

and

$$(x_0 - \bar{x}_1) \parallel (\bar{x}_1 - \bar{x}_2) \parallel \cdots \parallel \bar{x}_{n_2-1} - x_{n_1} \parallel \bar{p}_1 \parallel \bar{p}_2 \parallel \cdots \parallel \bar{p}_{n_2}$$

should be satisfied. Thus, we have $(x_0 - x_{n_1}) \parallel K_0$ and $(x_0 - x_{n_1}) \parallel \bar{K}_0$ which means

$$x_0 = x_{n_1}. \quad (4.4)$$

If one chooses x_0 as an origin of coordinates, all x_i lie along the light cone parallel to K_0 and all \bar{x}_i along \bar{K}_0 as shown in Fig. 4. It is interpreted that a hole position x_i is in $g_{p_i}(x_{i-1} - x_i)$ of $g_{p_i}(x_{i-1} - x_i)g_{p_{i+1}}(x_i - x_{i+1})$ and a particle position x_i in $g_{p_{i+1}}(x_i - x_{i+1})$, and that a hole catches a

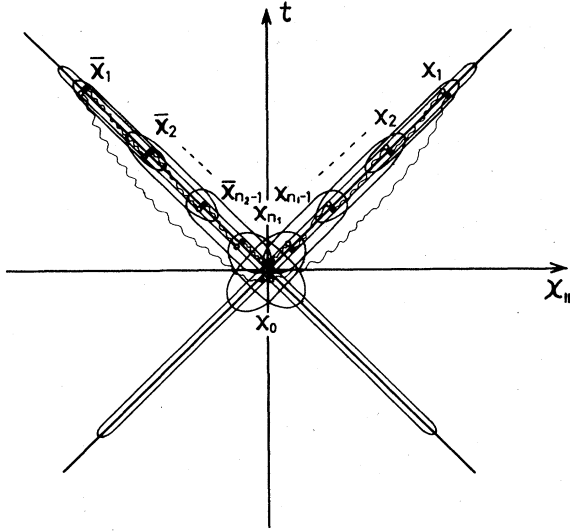


FIG. 4. Space-time configurations diagram in the overlap integral. x_i , \bar{x}_i denote space-time points where a particle and its hole are created. The wavy line between a particle and a hole shows interactions to develop into a meson.

particle to make a meson. Even if a particle is distant from a hole, they can be combined to make a meson when their energy is high enough so that they are bound in a tunnel.

Therefore the situation is as follows. A virtual photon creates a quark and an antiquark with momenta $K_0 = (W/2)(1, -\vec{e})$ and $\bar{K}_0 = (W/2)(1, \vec{e})$ at $x_0 = t_0 = 0$. At the same space-time position a quark and its hole are created with zero-energy momentum. A link of interactions subsequently develops particle-hole dissociation at several space-time positions on a light cone. The dissociation takes place at any position propagated along the jet axis with light velocity and the positions line up on the right- and left-hand side of the origin as

$$\vec{x}_i = -\vec{e}t_i \text{ or } \vec{x}_i = \vec{e}t_i, \quad (4.5)$$

with $|\vec{x}_i| = t_i$, $|\vec{x}_i| = \bar{t}_i$. Any quark with momentum $K_i = |\vec{K}_i|(1, -\vec{e})$ and hole with $-K_j = -|\vec{K}_j|(1, -\vec{e})$ can interact with each other to make a meson with momentum $p = K_i - K_j$ if the combined energy is positive and if two space-time positions (t_i, \vec{x}_i) and (t_j, \vec{x}_j) are close enough to be a bound state. The latter condition is expressed as

$$|t_i - t_j| < \frac{|\vec{p}|}{\sqrt{2}\eta}. \quad (4.6)$$

A quark on the right-hand light cone cannot catch a hole on the left-hand light cone to make a meson or vice versa because their relative space-time points do not lie on light cone but are spacelike.

Our many-particle system is described by multiple time such that each particle has its individual time. It is, therefore, impossible to describe the process in terms of a common time. Even though there is a difference between a common-time description and ours in interpretation, the space-time structure stated above just corresponds to the "inside-outside" process. Casher, Kogut, and Susskind³ discussed in the common-time description that the "inside-outside" process is more favorable in understanding jet formation than the "outside-inside" one.

V. SOME OBSERVABLE EFFECTS

A. Sea-quark diagrams

We have two distinct models depending on the value of ξ . For small ξ , momenta in a jet have to correlate with each other for each tunnel to include the crossed point B in Fig. 2, since the length of a tunnel is given by $\xi|\vec{p}_i|$. This leads to the strong ordering of meson momenta (SOCM). In the case of rather large ξ , on the other hand, it is easy for each tunnel to arrive at point B , so that the correlation of meson momenta is very weak (UCJM). To discriminate between two models by experiment, it is interesting to consider loop diagrams (Fig. 5) other than Fig. 1. We call Fig. 5 a sea-quark diagram in the sense that the " γ " line is not directly connected to the valence quark in a target hadron. The momentum diagram corresponding to Fig. 5 is now depicted in Fig. 6. The tunnel of the incident particle lies along OA . The T jet is divided into two parts, AB and DO , while the " γ " jet lies along BC . The overlap of BS amplitudes takes place in a small region around the point B . It is noted that there is a gap DB between the crossed point B and the tunnels along OD where the gap is given by $DB = Wx_B/[2(1-x_B)]$.

In the SOCM this diagram does not contribute much to the production amplitude if the gap DB is large. A rough estimation is done for the condition such that the diagram (Fig. 5) is very suppressed as compared to Fig. 1; $DB/p_i \gg 1/\alpha_i - \frac{1}{2} > \frac{1}{2}$ for any i . This leads to⁸

$$x_B \gg \frac{1}{3}. \quad (5.1)$$

In this region, Fig. 1 is the only dominant diagram and the cascade description is well satisfied. In the region $x_B \leq \frac{1}{3}$, on the other hand, the gap DB becomes small and the diagram (Fig. 5) has a non-negligible contribution. Since the T jet is composed of two parallel jets in this case and there is no ordering relation among momenta along AB and DO , the final momentum states have interferences and we cannot arrive at a cascade

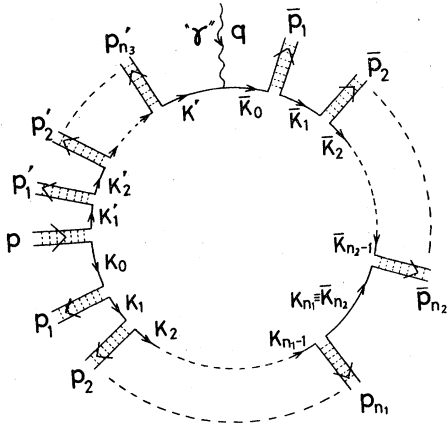


FIG. 5. Sea-quark diagram for n -meson production in a lepton-meson scattering. p denotes the incident-meson momentum, p_i, \bar{p}_i, p'_i the final-meson momenta and K_i, \bar{K}_i, K'_i the internal-line-quark momenta ($K_{n1} = \bar{K}_{n2} = 0$).

interpretation.

In the SOCM, therefore, we have interesting phenomena in the momentum distributions of the T jet. When one observes x_F distribution of a pion ($p = Wx_F/2$) in $l+h-l'+\pi$ anything, it is expected that the distribution pattern changes as x_B goes below $\frac{1}{3}$. The x_F distribution pattern in the “ γ ” jet, on the other hand, does not change at all. The situation in the UCJM is quite different from that in the SOCM. For large ξ it is easy for each tunnel on the OD line to arrive at the crossed point B except when $x_B \sim 1$. Therefore, the x_F distribution pattern does not change in both T and

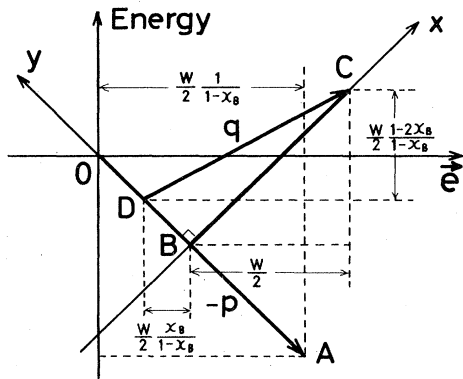


FIG. 6. Momentum diagram corresponding to Fig. 5. $AO = p$ and $DC = q$ represent four-momenta for the incident meson and “ γ ” in the c.m.s., respectively. The incident meson’s tunnel lies along OA and the produced meson’s tunnels lie along $AB, BC,$ and DO lines in $(-K_1)$ space with $AB = K_0 = \sum_i p_i = (Wa/2)(1, -\vec{e})$, $BC = \bar{K}_0 = \sum_i \bar{p}_i = (W/2)(1, \vec{e})$, $DO = \sum_i p'_i = [W(1-a)/2](1, -\vec{e})$, and $DB = K' = \{Wx_B/[2(1-x_B)]\}(1, -\vec{e})$, where $\vec{e} = \vec{q}/|q|$ and $0 \leq a \leq 1$.

“ γ ” jets when x_B does. It is said that in the SOCM the sea-quark diagram contributes to the production cross section in the small- x_B region and that in the UCJM it brings additional interference effects to the T jet at any x_B value.

B. Momentum distributions in the “ γ ” jet

In the SOCM there are interesting observable quantities in the “ γ ” jet for the final-momentum distributions,

$$\Gamma(\bar{\alpha}_1)\Gamma(\bar{\alpha}_2) \cdots \Gamma(\bar{\alpha}_{n-1})d\bar{\alpha}_1 d\bar{\alpha}_2 \cdots d\bar{\alpha}_{n-1},$$

in a cubic region $0 < \bar{\alpha}_i < 1$, provided that the trace factor T_μ does not have sharp momentum dependence as compared to $\Gamma(\bar{\alpha})$. (See Sec. VI.) If one picks up the two fastest moving particles, the leading and the next one with momentum \bar{p}_1, \bar{p}_2 in “ γ ” jet inclusively, $d^2\sigma/d\bar{\alpha}_1 d\bar{\alpha}_2$ has a symmetric distribution in $\bar{\alpha}_1 = 2\bar{p}_1/W$ and $\bar{\alpha}_2 = 2\bar{p}_2/[W(1-2\bar{p}_1/W)]$ space. Furthermore, F becomes a function of only one variable $X = (1\sqrt{\bar{\alpha}_1 - \frac{1}{2}})^2 + (1\sqrt{\bar{\alpha}_2 - \frac{1}{2}})^2$ if Eq. (2.14) is a good approximation. In the UCJM, on the other hand, there is no correlation among \bar{p}_1 and \bar{p}_2 so that Feynman’s scaling variables \bar{x}_1 and \bar{x}_2 become good observables. Let the two fastest particles in neutrino reaction be π^+ and π^- with \bar{x}_1 and \bar{x}_2 , respectively. In the case where the total charge of the “ γ ” jet is zero, π^+ and π^- are distributed symmetrically in (\bar{x}_1, \bar{x}_2) space. This is in contrast with the SOCM, where the distributions in $\bar{x}_1 > \bar{x}_2$ region are much more probable than those in the other region.

Let us take an example $\nu + N \rightarrow \mu^- + N + n\pi$ to consider charge distributions. As far as the “ γ ” jet is concerned, $\nu + N$ reactions are quite similar to $\nu + \text{meson}$ reactions.⁸ Since the “ γ ” jet is produced by the “decay” of a u quark created through “ γ ”- d quark interaction, the allowed combination of the fastest and second fastest pions are (π^+, π^0) , (π^+, π^-) , (π^0, π^+) , or (π^0, π^0) in the SOCM. Therefore, the combination (π^+, π^+) , (π^-, π^+) , or (π^-, π^+) of charged pions will be very suppressed as compared to the allowed ones. In the UCJM any combination comes out with almost equal weight except for some $SU(2)$ factors. Experimental data⁷ appear to favor the uncorrelated Monte Carlo calculation (UMC) which is almost similar to our UCJM. Since there is a possibility that vector mesons are produced, further checks will be needed to confirm the above discussion.

C. Mass effects

So far, outgoing mesons have been considered lightlike with enough high energy such that $E \sim m_\perp e^y$, $p_\parallel \sim m_\perp e^y$. Consider some soft mesons that are emitted with momenta comparable to m_\perp . This, however, reduces O_n considerably because

the centers of these meson's tunnels shift from the light cone (AB or BC line) in Fig. 2. When incoming or outgoing hadrons are replaced by heavier ones, O_n is also reduced at such energies, as their masses are not negligible compared to their momenta. We understand, in this sense, a suppression mechanism of the heavy-particle production rate. It is also said that one of the heaviest outgoing hadrons (K , D , ψ , T , etc.) in a jet must be produced with the highest momentum to suppress the mass effect.

It is stated in the SOCM that the minimal momentum p_{n_1} (\bar{p}_{n_2}) in a jet should be cut off at some value μ larger than m_1 ;

$$p_{n_1} = (W/2)(1 - \alpha_1)(1 - \alpha_2) \cdots (1 - \alpha_{n_1-1}) \geq \mu.$$

Under this condition and at $x_B \geq \frac{1}{3}$, $\prod_{i=1}^{n_1-1} \Gamma(\alpha_i)$ becomes maximum at $\alpha_1 = \alpha_2 = \cdots = \alpha_{n_1-1} = \alpha$, where $\alpha = 1 - (2\mu/W)^{1/(n_1-1)}$. We have equal spacing in y distributions

$$y_{i-1} - y_i \simeq (n_1 - 1)^{-1} \ln(W/2\mu) \quad (5.2)$$

due to $p_i = (W/2)(1 - \alpha)^{i-1} \alpha$.

VI. DISCUSSIONS AND CONCLUSIONS

The assumption that every incoming or outgoing hadron has a structure in a finite space-time region inside itself has played a crucial role in understanding jet phenomena. We have studied what physical consequences result under this assumption by considering a simple loop diagram. It is difficult at present to solve for the BS amplitude under a confinement potential because we do not know of the relativistic confinement potential. The above assumption on the BS amplitude, however, seems natural because it should be normalized to a finite value.

The value of ξ , which is one of the parameters used to define an elliptic region inside a moving hadron plays an essential role in leading to two distinct models. For small ξ we have the SOCM, which is well described by a classical stochastic process for quark cascade. For large ξ there are less momentum correlations among final hadron states and we have the uncorrelated jet model which is essentially equivalent to the one done by an UMC calculation. If meson momenta in a jet have completely symmetric distribution, we obtain a selection rule for the number of charged and neutral pions produced. Though we are not convinced whether or not asymmetric parts come from the trace factor in spinor space, it is interesting to look for meson-number dependence on the production cross sections.

The real world in jet phenomena may be intermediate between the SOCM and UCJM. It is, therefore, interesting to see which model real

phenomena favor. Several observable effects to distinguish between these two models were presented. It is hoped that detailed experiment will be done in this connection.

The overlap integral in relative-momentum space has been translated into space-time descriptions. Though a multiple-particle system is described by multiple time in the relativistic quantum field theory, it is clarified that our model corresponds just to the "inside-outside" model proposed by Casher, Kogut, and Susskind³ in a common-time theory which is reasonable in understanding the materialization process.

Finally, we give a short comment on the momentum dependence in the trace factor T_μ . A detailed calculation is given for $e^+ - e^-$ scattering in Ref. 6. To get numerical results of the production cross section to compare with experiment, we have to calculate T_μ in lepton-nucleon scattering explicitly. These tedious calculations remain as a future task. Though we do not calculate it explicitly in lepton-meson scattering, the highest energy-dependent term is estimated. The similar estimation is applied to T_μ in lepton-nucleon scattering.⁸ The spinor matrix in a trace factor has two origins. One comes from quark propagators $S_F(K_i)$ and the other from the BS amplitude $S(p_i)$ in spinor space. When S_F is written as $S_F S_F^{-1} S_F$, two S_F 's in both sides are absorbed into two neighboring BS amplitudes.¹⁵ $S(p_i)$ is given as $(1 + \gamma \cdot p_i / \kappa) \gamma_5$ for pseudoscalar mesons; for example. Then the trace is calculated for a multiple of several S_F^{-1} , S , and γ matrix at the quark-" γ " vertex. Any momentum coming from the " γ "-jet part in the loop diagram is almost proportional to $\vec{K}_0 = (W/2)(1, \vec{e})$ and the one from the T jet is proportional to $\vec{K}_0 = (W/2)(1, -\vec{e})$. Since a product $\not{p}_i \not{p}_j$ or $\not{p}_i \not{p}_j$ in a jet vanishes in this approximation, we only have bilinear terms of $\not{p}_i \vec{p}_j$ as a highest power in the trace. In the SOCM, T_μ does not have much momentum dependence compared to $\Gamma(\alpha)$ which is strongly dependent on momentum, because we can take a strongly ordering limit in T_μ such that the leading particle in a jet carries most of the momenta. Therefore the trace term does not have much effect in changing the distribution. In the UCJM, the amplitude coming from the overlap integral has a weak dependence on each momentum. Thus, there may be a possibility for the trace factor to disturb the momentum distribution.

ACKNOWLEDGMENT

The authors would like to thank the theoretical groups of the Department of Physics and College of Liberal Arts at Kobe University for helpful discussions.

- ¹R. D. Field and R. P. Feynman, Nucl. Phys. B136, 1 (1978), and references cited therein. For early works on jet models, see S. D. Drell, D. J. Levy, and T. M. Yan, Phys. Rev. 187, 2159 (1969); Phys. Rev. D 1, 1617 (1970); N. Cabibbo, G. Parisi, and M. Testa, Lett. Nuovo Cimento 4, 35 (1970); J. D. Bjorken and S. J. Brodsky, Phys. Rev. D 1, 1416 (1970); S. M. Berman, J. D. Bjorken, and J. B. Kogut, *ibid.* 4, 3388 (1971); R. P. Feynman, *Photon-Hadron Interactions* (Benjamin, New York, 1972). See also Ref. 3.
- ²Field and Feynman, Ref. 1.
- ³A. Casher, J. Kogut, and L. Susskind, Phys. Rev. Lett. 31, 792 (1973); Phys. Rev. D 10, 732 (1974); J. Kogut, D. K. Sinclair, and L. Susskind, *ibid.* 7, 3637 (1973); J. D. Bjorken and J. Kogut, *ibid.* 8, 1341 (1973); J. D. Bjorken, in *Current Induced Reactions*, proceedings of the Summer School on Theoretical Particle Physics, Hamburg, 1975, edited by J. G. Korner, G. Kramer, and D. Schildknecht (Springer, New York, 1976), p. 93; S. J. Brodsky and N. Weiss, Phys. Rev. D 16, 2325 (1977); Y. Zarmi, Nucl. Phys. B134, 521 (1978).
- ⁴J. F. Gunion, S. J. Brodsky, and R. Blankenbecler, Phys. Rev. D 6, 2652 (1972). A general reference is D. Sivers, S. J. Brodsky, and R. Blankenbecler, Phys. Rep. 23, 1 (1976). This also includes a more detailed reference list to the early works. See also P. V. Landshoff and J. C. Polkinghorne, Phys. Rev. D 8, 927 (1973); M. Schmidt, *ibid.* 9, 408 (1974); A. Le Yaouanc, L. Oliver, O. Pène, and J.-C. Raynal, *ibid.* 12, 2137 (1975); Y. S. Kim and M. E. Noz, *ibid.* 15, 335 (1977).
- ⁵Y. S. Kim, M. E. Noz, and S. H. Oh, University of Maryland CTP Tech. Report No. 79-033, 1978 (unpublished); Y. S. Kim and M. E. Noz, Hadronic J. 2, 460 (1979).
- ⁶T. Kitazoe and S. Hama, Phys. Rev. D 19, 2006 (1979).
- ⁷Jet properties of neutrino-induced reactions were studied, for example, by J. Bell, C. T. Coffin, R. N. Diamond, H. T. French, W. C. Louis, B. P. Roe, R. T. Ross, A. A. Seidl, J. C. Vander Velde, E. Wang, J. P. Berge, D. V. Bogert, F. A. DiBianco, R. Endorf, R. Hanft, C. Kochowski, J. A. Malko, G. I. Moffatt, F. A. Nezrick, W. G. Scott, W. Smart, R. J. Cence, F. A. Harris, M. Jones, M. W. Peters, V. Z. Peterson, V. J. Stenger, G. R. Lynch, J. P. Merriner, and M. L. Stevenson, Phys. Rev. D 19, 1 (1979); P. C. Bosetti, H. Deden, M. Deutschman, P. Fritze, H. Grässler, F. J. Hasert, J. Morfin, R. Schulte, K. Schultze, H. Seyfert, K. Böckmann, H. Emans, C. Geich-Gimbel, R. Hartmann, G. Heilmann, A. Keller, T. P. Kokott, R. Künne, W. Meincke, B. Nellen, R. Pech, D. C. Cundy, J. Figiel, A. Grant, D. Haidt, P. O. Fulth, G. T. Jones, D. J. Kocher, D. R. O. Morrison, E. Pagiola, L. Pare, C. Peyrou, V. Peterson, P. Porth, P. Schmid, W. G. Scott, E. Simopoulou, A. Vayaki, H. Wachsmuth, K. L. Wernhard, S. Banerjee, K. W. J. Barnham, R. Beusel-inck, I. Butterworth, S. J. Chima, E. F. Clayton, D. B. Miller, K. J. Powell, C. L. Davis, R. Grossmann, R. McGow, J. H. Mulvey, G. Myatt, D. H. Perkins, R. Pons, D. Radojicic, P. Renton, B. Saitta, V. J. Stenger, V. Baruzzi, M. Bloch, M. De Beer, W. Hart, Y. Sacquin, B. Tallini, and D. Vignaud, Nucl. Phys. B149, 13 (1979).
- ⁸T. Kitazoe and T. Morii, Nucl. Phys. B (to be published).
- ⁹J. L. Newmeyer and D. Sivers, Phys. Rev. D 9, 2592 (1974).
- ¹⁰D. J. Gross and F. Wilczek, Phys. Rev. Lett. 25, 1343 (1973); H. D. Politzer, *ibid.* 25, 1346 (1973).
- ¹¹Our uncorrelated jet model is not the same one as Van Hove discussed before. L. Van Hove, Nuovo Cimento 28, 798 (1963).
- ¹²See, for example, the Appendix of Bell *et al.*, Ref. 7.
- ¹³As is discussed later, Δ is closely related to $\langle p_{\perp} \rangle$ which is very small (≈ 0.3 GeV). [See Eq. (2.11).]
- ¹⁴F. Zachariasen and G. Zweig, Phys. Rev. 160, 1326 (1967); C. E. DeTar, Phys. Rev. D 3, 128 (1971); C. J. Hamer and R. F. Peierls, *ibid.* 8, 1358 (1973).
- ¹⁵T. Kitazoe and T. Teshima, Nuovo Cimento 57A, 497 (1968).